Brain Research 1791 (2022) 147995

Contents lists available at ScienceDirect

Brain Research

journal homepage: www.elsevier.com/locate/brainres

The effect of central growth hormone action on hypoxia ventilatory response in conscious mice

Talita M. Silva [a], Frederick Wasinski [a], Karine C. Flor [a], Edward O. List [b], John J. Kopchick [b], Ana C. Takakura [c], Jose Donato Jr. [a], Thiago S. Moreira [a,*]

[a] Department of Physiology and Biophysics, Instituto de Ciencias Biomedicas, Universidade de Sao Paulo (USP), 05508-000 São Paulo/SP, Brazil
[b] Edison Biotechnology Institute and Heritage College of Osteopathic Medicine, Ohio University, Athens, OH 45701, USA
[c] Department of Pharmacology, Instituto de Ciencias Biomedicas, Universidade de Sao Paulo (USP), 05508-000 São Paulo/SP, Brazil

ARTICLE INFO

Keywords:
Hypoxia
Peripheral chemoreflex
Brainstem
Growth hormone

ABSTRACT

Growth hormone (GH)-responsive neurons regulate several homeostatic behaviors including metabolism, energy balance, arousal, and stress response. Therefore, it is possible that GH-responsive neurons play a role in other responses such as CO_2/H^+-dependent breathing behaviors. Here, we investigated whether central GH receptor (GHR) modulates respiratory activity in conscious unrestrained mice. First, we detected clusters of GH-responsive neurons in the tyrosine hydroxylase-expressing cells in the rostroventrolateral medulla (C1 region) and within the locus coeruleus (LC). No significant expression was detected in phox2b-expressing cells in the retrotrapezoid nucleus. Whole body plethysmography revealed a reduction in the tachypneic response to hypoxia ($FiO_2 = 0.08$) without changing baseline breathing and the hypercapnic ventilatory response. Contrary to the physiological findings, we did not find significant differences in the number of fos-activated cells in the nucleus of the solitary tract (NTS), C1, LC and paraventricular nucleus of the hypothalamus (PVH). Our finding suggests a possible secondary role of central GH action in the tachypneic response to hypoxia in conscious mice.

1. Introduction

In the respiratory physiology and the regulation of pulmonary ventilation, the tensions of oxygen and carbon dioxide are considered controlled variables. Disturbances in partial pressure of O_2 (PaO_2) or partial pressure of CO_2 ($PaCO_2$) are detected by the peripheral and central chemoreceptors, located in the carotid bodies and brainstem, respectively. In the brainstem, afferent inputs from both categories of chemoreceptors are processed and integrated with other information to yield a final command to the respiratory motoneurons. Numerous studies have been devoted to localizing and characterizing the elements of the brainstem respiratory neural network (Ashhad et al., 2022; Del Negro et al., 2018). Within the medulla oblongata, respiratory neurons are mainly concentrated within the nucleus tractus solitarius (NTS) and in a ventrolaterally located cell column, extending approximately from the highest cervical level to the retrotrapezoid nucleus (Del Negro et al., 2018; Guyenet and Bayliss, 2015). Besides the role of the brainstem in controlling breathing activities, the forebrain, especially the hypothalamus, also contains an important cluster of neurons involved in breathing regulation. Therefore, brain regions responsible for arousal, metabolic homeostasis and respiratory chemoreception may share common sensory modalities and anatomical connections that promote coordinated regulation of respiratory and metabolic activity.

Recent studies have shown that hypothalamic growth hormone (GH)-responsive neurons regulate several homeostatic behaviors including metabolism, energy balance, arousal, and stress response (Donato et al., 2021). Thus, it is possible that GH-responsive neurons may also be involved in the control of other neurological based actions such as CO_2/H^+-dependent breathing behaviors. Only correlative data exists on the interactions of GH and breathing. That is, patients with obstructive sleep apnea (OSA) experience hypoxia, and GH secretion is decreased (Lanfranco et al., 2010; Li et al., 2011; Nair et al., 2013). In addition, several brainstem areas related to breathing regulation, including the NTS, locus coeruleus (LC), and the catecholaminergic cells in the ventrolateral medulla (C1 region) contain GH-responsive neurons (Furigo et al., 2017; Wasinski et al., 2020; Wasinski et al., 2021).

* Corresponding author at: Department of Physiology and Biophysics, Instituto de Ciencias Biomedicas, Universidade de Sao Paulo, Av. Prof. Lineu Prestes, 1524, 05508-000 São Paulo, SP, Brazil.
E-mail address: tmoreira@icb.usp.br (T.S. Moreira).

https://doi.org/10.1016/j.brainres.2022.147995
Received 13 May 2022; Received in revised form 23 June 2022; Accepted 26 June 2022
Available online 30 June 2022

However, the effects of central GH action on resting ventilation and on the chemosensory control of breathing are unknown.

Therefore, in the present study, we investigated whether GH receptor (GHR) in CNS neurons modulates respiratory activity in conscious unrestrained mice. We also determined whether hypoxia-induced changes in neuronal activity were disrupted in neuron-specific GHR knockout (KO) mice (nGHR KO).

2. Materials and methods

2.1. Animals

GH-responsive neurons and hypoxia-induced GH secretion were studied using 12-week-old C57BL/6 male mice. To generate mice carrying genetic ablation of GHR specifically in neurons, we bred mice carrying loxP-flanked *Ghr* alleles (List et al., 2013) with Nestin-Cre mice (The Jackson Laboratory, Bar Harbor, ME; RRID: IMSR_JAX:006660)]. After successive matings to establish a mouse colony homozygous for the loxP-flanked *Ghr* alleles, we generated the Cre-expressing conditional KO mice used in the experiments (nGHR KO) and their respective littermate controls that did not carry the Cre transgenes ($Ghr^{flox/flox}$ mice). In all experiments, approximately 15-week-old male mice in a C57BL/6 background were used. To confirm the neuron-specific GHR ablation, brain samples were collected from control and nGHR KO mice and the *Ghr* mRNA levels were assessed by quantitative real-time PCR, as previously described (Wasinski et al., 2021).

For the study, mice were weaned at 3 weeks of life, and their mutations confirmed by PCR using DNA previously extracted from the tail tip (REDExtract-N-Amp Tissue PCR Kit, Sigma-Aldrich, St. Louis, MO). Mice had *ad libitum* access to regular rodent chow and filtered water. The experiments were approved by the Ethics Committee on the Use of Animals of the Institute of Biomedical Sciences at the University of São Paulo and were performed in accordance with the ethical guidelines of the Brazilian College of Animal Experimentation.

2.2. Hypoxia protocol

Fos-like immunoreactivity evoked by hypoxia was performed in conscious, unrestrained adult mice. The day before the experiment, animals were kept in a plexiglass chamber (0.5 L) that was flushed continuously with room air at a rate of 0.5 L/min, to allow them to become acclimated to the environmental stimuli associated with the chamber and to minimize unspecific Fos expression. Mice were first acclimated for 45 min in the chamber and after subjected to acute hypoxia (AH; $FiO_2 = 0.08$), balanced with N_2 or normoxia ($FiO_2 = 0.21$) for 3 h, as previously demonstrated (Berquin et al., 2000; King et al., 2015; Silva et al., 2016). At the end of the stimulus, mice were immediately and deeply anesthetized with pentobarbital (60 mg/kg, i.p.) and transcardially perfused. All experiments were performed at room temperature (24–26 °C).

2.3. Plethysmography/chemoreflex analysis

Respiratory rate (f_R, breaths/min) and tidal volume (V_T, μl/g) were recorded from unrestrained mice by whole-body flow barometric plethysmograph as described in detail previously (Bartlett and Tenney, 1970; Malan, 1973; Czeisler et al., 2019). Mice were acclimatized to the plethysmography chambers 2–3 days prior to the experiments. On an experimental day, mice were placed in a plexiglass recording chamber (0.5 L) that was flushed continuously with room air (normoxia) at a rate of 0.5 L/min. During ventilation measurements, the flow was interrupted, and the chamber closed for 2 min after normoxia or hypoxia. The peripheral chemoreflex activation was induced by hypoxia, lowering the O_2 concentration in the inspired air to a level of 8% for 10 min. The pressure signal was amplified, filtered, recorded, and analyzed offline using Powerlab software (Powerlab 16/30, ML880/P, ADInstruments, NSW, Australia). The temperature was measured using Thermistor Pod (ML 309, ADInstruments, NSW, Australia). Changes in the f_R, V_T, and minute ventilation (V_E) ($f_R \times V_T$; μl/min/g) were averaged and expressed as means ± SEM. To account for differences in body size, breath volumes were also normalized to body weight.

2.4. Detection of GH-responsive neurons/ histology and immunofluorescence

To detect GH-responsive neurons, 12-week-old wild-type male mice received an intraperitoneal (i.p.) injection of 20 μg/g of body weight of porcine pituitary GH (from Dr. A.F. Parlow, National Hormone and Pituitary Program, Torrance, CA) and were perfused 60 to 90 min later. Saline-injected mice were used as negative controls to demonstrate the very low basal pSTAT5 expression observed in mice without GH stimulus (Furigo et al., 2017; Wasinski et al., 2021).

For the perfusion, mice were deeply anesthetized with pentobarbital (60 mg/kg, i.p.), then injected with heparin (0.1 ml, intracardially) and finally perfused through the ascending aorta with 50 ml of phosphate-buffered saline (PB - pH 7.4), followed by 100 ml of 4% phosphate-buffered paraformaldehyde (0.1 M, pH 7.4). The brains were removed from the skull, cryoprotected by overnight immersion in a 20% sucrose solution in phosphate-buffered saline at 4 °C, sectioned in the coronal plane at 30 μm on a sliding microtome, and stored in cryoprotectant solution (20% glycerol plus 30% ethylene glycol in 50 mM phosphate buffer, pH 7.4) at −20°C awaiting histological processing. All histochemical procedures were done using free-floating sections according to previously described protocols.

Free-floating brain sections were subjected to a double immunofluorescence staining protocol to check a possible co-localization of pSTAT5 and markers for neurons or astrocytes. Brain sections were rinsed in KPBS, followed by pretreatment in water solution containing 1% hydrogen peroxide and 1% sodium hydroxide for 20 min. Sections were incubated in 0.3% glycine and 0.03% lauryl sulfate for 10 min each. Next, sections were blocked in 3% normal donkey serum (Jackson Laboratories, West Grove, PA) for 1 h, followed by incubation for 40 h at 4 °C in cocktails of either rabbit anti-$pSTAT5^{Tyr694}$ (Cell Signaling Technology, Beverly, MA; 1:1000) and polyclonal anti-Phox2b raised in rabbit (1:800 dilution; gift from J. F. Brunet, Ecole Normale Superieure, Paris, France), anti-tyrosine hydroxylase (TH) raised in mouse (MAB 318; Millipore; dilution 1:1000), or anti-glial fibrillary acidic protein (GFAP) raised in mouse (Millipore; 1:1000) primary antibodies. Fos protein was detected using anti-Fos raised in rabbits (Ab-5; Calbiochem, Darmstadt, Germany; dilution 1:10,000). Subsequently, sections were rinsed in KPBS and incubated for 2 h in $AlexaFluor^{594}$-conjugated anti-rabbit IgG, $AlexaFluor^{488}$-conjugated anti-mouse IgG, and $AlexaFluor^{488}$-conjugated anti-mouse IgG antibodies (1:1500, Jackson Laboratories). The slides were coverslipped with Fluoromount G containing DAPI (Electron Microscopic Sciences, Hatfield, PA).

2.5. Cell counting, imaging, and data analysis

Photomicrographs were acquired using a Zeiss Axioimager A1 microscope (Zeiss, Munich, Germany). The locations of TH and Fos immunoreactivity in the A1/C1 region were plotted in sections from 8.0 to 6.36 mm caudal to bregma and four sections were analyzed per animal (bregmas −8.0, −7.76, −7.20, −6.84 mm); the ventral quadrants were plotted, and profile counts reflect an average and total number of cells in both sides of the medulla. The TH and Fos-ir neurons within the caudal aspect of the nucleus of the solitary tract (cNTS) and dorsal motor nucleus of the vagus (DVMN) were plotted in sections from −7.92 to −7.56 mm caudal to bregma and three sections were analyzed per animal (bregmas −7.92, −7.76, −7.64 mm). LC was plotted in sections from −5.68 to −5.34 mm caudal to bregma and two sections were analyzed per animal (bregmas −5.40, −5.52) and PVH from −0.94 to −0.70 mm, and two sections were analyzed per animal (bregmas −0.94,

−0.82).

The Image J Cell Counter software (https://rsb.info.nih.gov/ij) was used to manually count the number of single- or double-labeled cells, and the (Paxinos and Franklin, 2012) atlas was used as a neuroanatomical reference.

2.6. Evaluation of GH secretion

Tail-tip blood samples (5 µl) were collected in 12-week-old C57BL/6 male mice before and after the hypoxia challenge. Immediately before the first sample collection, a small portion of the tail tip (1 mm) was cut with a surgical blade to allow the collection of small drops of blood. For each blood collection, mice were placed inside the cardboard tube and quickly held by the base of the tail. Using a 10 µl pipette, a 5 µl sample of whole blood was collected and transferred to 105 µl of PBS with 0.05% Tween-20 (PBS-T). After each blood collection, a fingertip pressure was gently applied to the tail tip to stop bleeding. Samples were immediately placed on dry ice and stored at −80 °C for later analysis. Blood GH levels were determined using an in-house highly sensitive sandwich enzyme-linked immunosorbent assay, as previously described (Wasinski et al., 2020).

2.7. Statistical analysis

Statistical analysis of the data was performed using GraphPad Prism software. All the data were expressed as means ± SEM and significance was set at $p < 0.05$ in a random-effect model. All data passed normality using the Shapiro-Wilk test and variance homogeneity was verified with the Brown-Forsythe test. Comparisons between the groups were performed using unpaired 2-tailed Student *t* test (Mann-Whitney test). Two-way repeated measurements ANOVA followed by Bonferroni post-test was used to analyze breathing parameters in control and nGHR KO mice.

3. Results

3.1. Distribution of GH-responsive cells in the brainstem respiratory areas

To detect GH-immunoreactive cells in the mouse brain, 12-week-old wild-type C57BL/6 male mice received an i.p infusion of porcine GH (pGH) and then were perfused 60 to 90 min later to detect pSTAT5 immunoreactivity. In the ventral respiratory column, we detected clusters of GH-responsive neurons in the RTN and preBötC (Fig. 1A–D). In the dorsal brainstem, pSTAT5 immunoreactivity was detected in the NTS (both in the caudal and intermediate aspects) and in the locus coeruleus (Fig. 1E–J). At the area postrema level, the DVMN also expresses high levels of pSTAT5 (Fig. 1G–H). The cholinergic neurons located in the nucleus ambiguus or in the motor nucleus of hypoglossal did not express pSTAT5 (Fig. 1C–F). Because the hypothalamus concentrates the largest numbers of GH-responsive neurons (Furigo et al., 2017; Wasinski et al., 2021), we noticed a high level of GH-expressing cells in the PVH (Fig. 1K–L). According to our analysis and previous studies (Quaresma et al., 2021; dos Santos et al., 2021), the pSTAT5 expression was spread all over the magno and parvocellular sub-regions. Saline-injected mice were used as negative controls and according to the former described experiments (Furigo et al., 2017; Wasinski et al., 2021), they exhibited practically no pSTAT5 expression in all these brain areas (Fig. 1).

To be more specific in terms of the phenotype of brainstem neurons, the next series of experiments were performed to evaluate the expression of pSTAT5 in phox2b or TH-expressing neurons in the brainstem of mice. We found that only 2 ± 1% of Phox2b-expressing neurons were responsive to GH in the NTS, and a higher number of Phox2b neurons in DVMN co-localize with GH (47 ± 12%) (Fig. 2A–C). As far as the TH-expressing cells in the brainstem, we observed that 54 ± 9% of TH-expressing cells in the C1 region and 95 ± 3% of TH-expressing cells of the LC were responsive to GH (Fig. 2D–F and J–L). GH-responsive

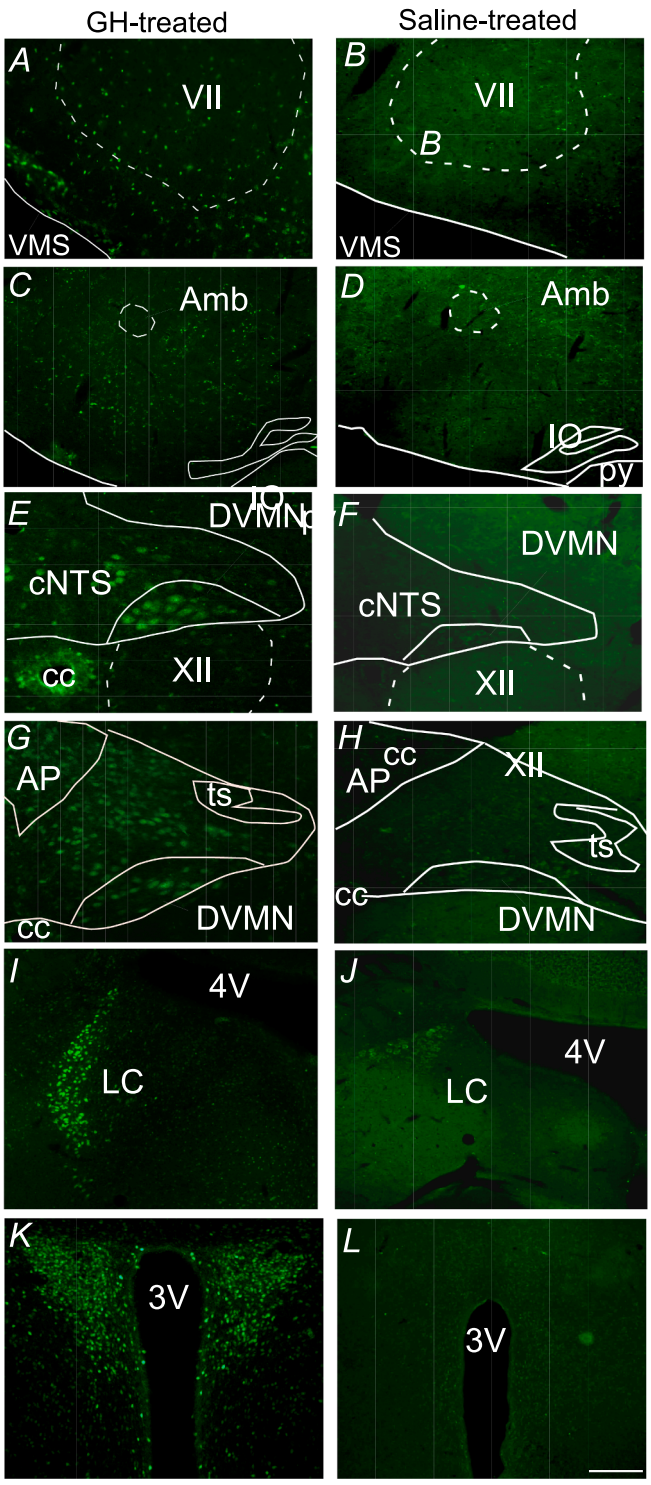

Fig. 1. Distribution of GH-responsive cells in the brainstem and hypothalamus. A-L) Cells expressing pSTAT5 immunoreactivity (pSTAT5-ir) in wild type (C57BL/6) mice that received an i.p. injection of GH (A, C, E, G, I and K) or saline (B, D, F, H, J and L) in the (A-B) parafacial respiratory region (pFRG - RTN), (C-D) preBötzinger complex, (E-H) nucleus of the solitary tract, (I and J) locus coeruleus, and (K-L) paraventricular nucleus of the hypothalamus (PVH). Abbreviations: Amb, nucleus ambiguous; AP, area postrema; cc, central canal; cNTS, caudal aspect of the nucleus of the solitary tract; DVMN, dorsal vagus motor nucleus; LC, locus coeruleus; IO, inferior olive; py, pyramid tract; ts, tractus solitarius; VMS, ventral medullary surface; 3 V, third ventricle; 4 V fourth ventricle; VII, facial motor nucleus; XII, hypoglossal motor nucleus. Scale bar in L = 200 µm (applied to all panels).

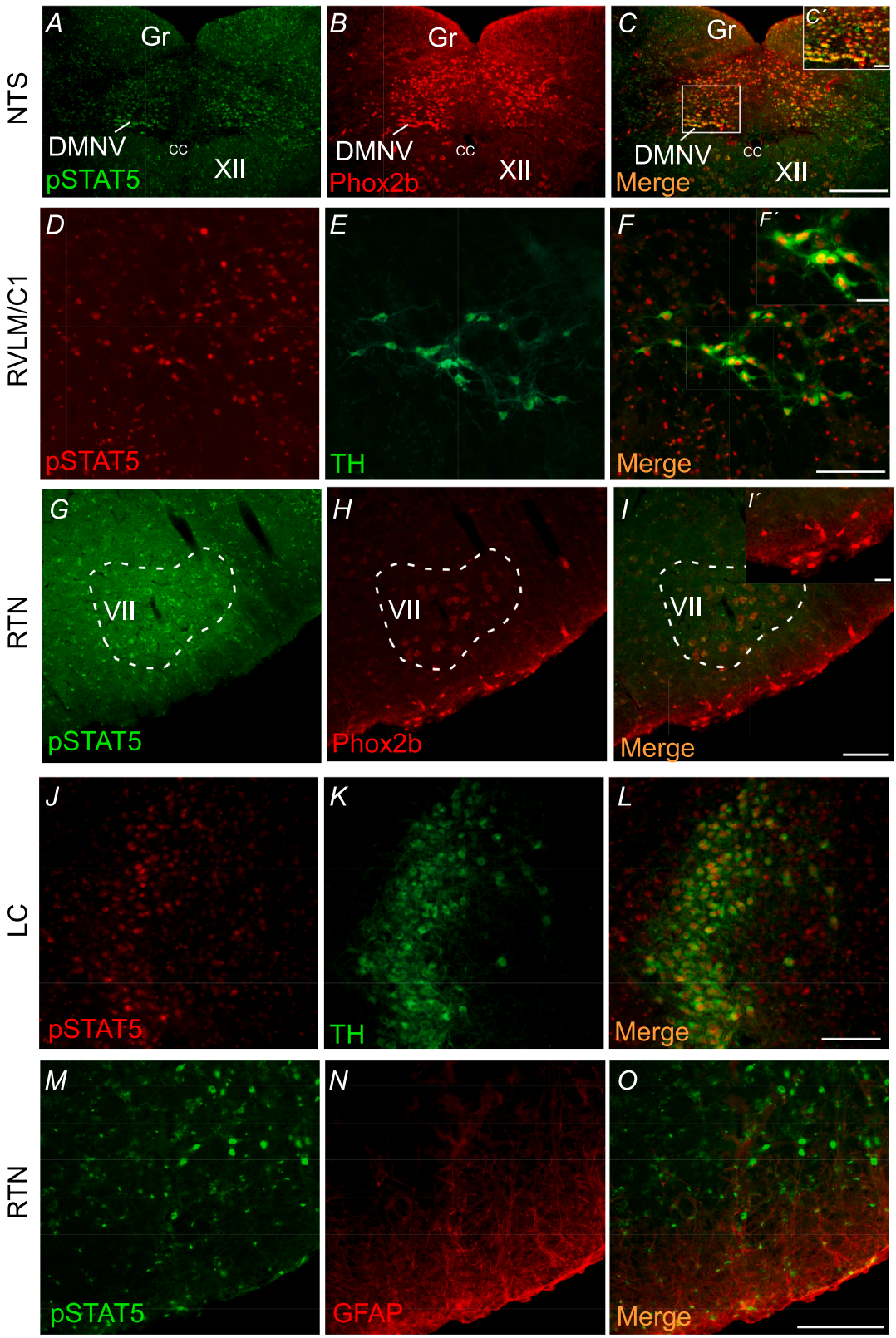

Fig. 2. Distribution of GH-responsive cells in the specific brainstem profiles. Immunohistochemistry for pSTAT5 was combined with Phox2b, TH, or GFAP, and differentially labeled cells were mapped in sections through the A-C) nucleus of the solitary tract (NTS); D-F) rostral ventrolateral medulla/C1 region (RVLM-C1); G-I and M−O) parafacial respiratory region/retrotrapezoid nucleus (RTN); J-L) locus coeruleus (LC), as indicated. The insets represent high magnification of the square depicted in Figures C, F and I. Scale bar: 0.5 mm in C (applied to A-C); 50 μm in C; 100 μm in F (applied to D-F); 40 μm in F́; 100 μm in I (applied to G-I); 20 μm in Í; 100 μm in L (applied to J-L); 100 μm in O (applied to M−O). Abbreviations: cc, central canal; DMNV, dorsal motor nucleus of the vagus; GR, gracile nucleus; VII, facial motor nucleus; XII, hypoglossal motor nucleus.

neurons in the ventral medullary surface (parafacial respiratory region – pF) did not co-localize with Phox2b (presumably RTN chemosensitive neurons) (Fig. 2G–I). We also analyzed if the expression of GH-responsive cells were co-localized with GFAP, as a marker of astrocytes, in the level of the parafacial respiratory region. We did not find colocalization of pSTAT5 and GFAP immunoreactive in the pF region (Fig. 2M–O).

To investigate the physiological role of central GHR signaling, a neuron specific GHR knockout mouse was produced (hereafter named as nGHR KO). Confirming the predominant expression of GHR in neurons, nGHR KO exhibited a 90% reduction in the brain expression of GHR mRNA (0.10 ± 0.01 vs. control: 1.00 ± 0.14 a.u; p = 0.0079; Mann-Whitney test) in comparison with controls.

3.2. Breathing responses in neuron specific nGHR KO mice

The following series of experiments were performed to evaluate the breathing patterns in 15-week-old control and nGHR KO unrestrained male mice.

No changes in baseline V_T (10.4 ± 0.93 vs. control: 10.6 ± 0.51 µl/g, P = 0.85]), f_R (200.4 ± 10.6 vs. control: 201.4 ± 6.9 breaths/min, P = 0.93]), V_E (2054.7 ± 119.2 vs. control: 2137 ± 93 µl/min/g, P = 0.59]), T_I (0.096 ± 0.0033 vs. control: 0.092 ± 0.0035 s, P = 0.44]), T_E (0.21 ± 0.017 vs. control: 0.21 ± 0.012 s, P = 0.86) and T_{TOT} (0.31 ± 0.017 vs. control: 0.31 ± 0.010 s, P = 0.99) were observed (Fig. 3A–F). Challenging the animals to 7% CO_2 (hypercapnia ventilatory response - HCVR) led to increased V_T (21.5 ± 1.8 vs. control: 18.67 ± 1.2 µl/g, [$F_{1,14}$ = 1.0, P = 0.31]), f_R (370.6 ± 17.4 vs. control: 357.6 ± 11 breaths/min, [$F_{1,14}$ = 1.1, P = 0.31]) and V_E (7894.7 ± 398.9 vs. control: 6667.8 ± 422.1 µl/min/g, [$F_{1,14}$ = 4.0, P = 0.06]), in both control and nGH KO mice (Fig. 3A–F). On the other hand, nGH KO mice exhibited a different response to 8% O_2 (hypoxia ventilatory response - HVR) when compared to controls, since a significant reduction in the tachypneic response (227 ± 16.4 vs. control: 267.9 ± 10 breaths/min, [$F_{1,15}$ = 8.6, P = 0.01]) was observed (Fig. 4B). This alteration was associated with an increase in T_E (0.19 ± 0.023 vs. control: 0.14 ± 0.008 s, [$F_{1,15}$ = 7.2, p = 0.01]), and T_{TOT} (0.3 ± 0.03 vs. control: 0.24 ± 0.01 s, [$F_{1,15}$ = 7.8, p = 0.01]), in comparison with controls (Fig. 4B and E–F).

We did not find significant changes in body temperature in both control and nGH KO mice (36.9 ± 0.2, vs. nGHR KO: 36.7 ± 0.2; *t*-test; p > 0.05). In addition, during the experiments, the mean chamber temperature was 26.3 ± 0.2 °C, and the mean room temperature was 25.3 ± 0.3 °C.

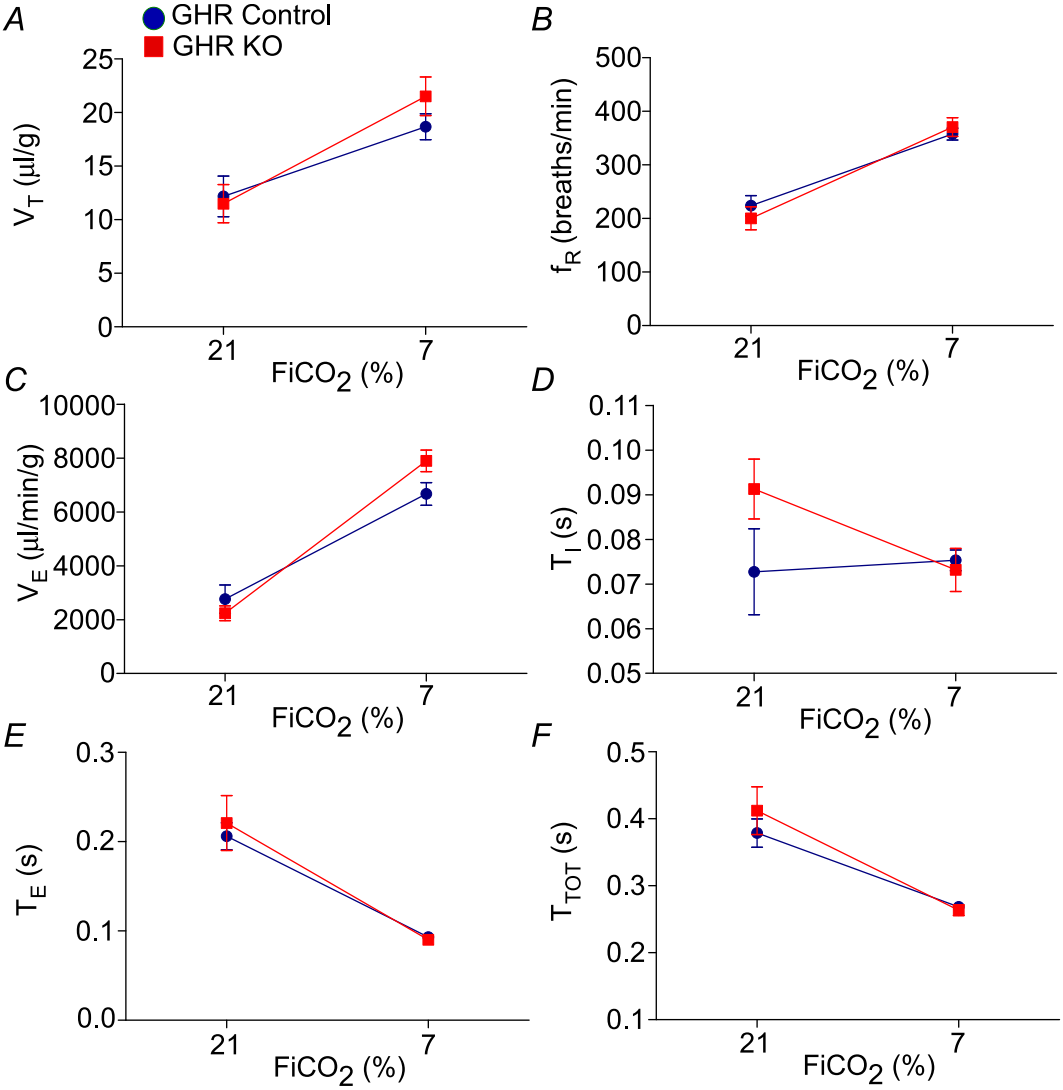

Fig. 3. GHR knockout mice do not have a change in the CO_2-stimulated breathing *in vivo*. Changes in A) tidal volume (V_T, µl/g); B) respiratory rate (f_R, breaths/min); C) minute ventilation (V_E, µl/min/g); D) inspiratory time (T_I, s); E) expiratory time (T_E, s), and F) total respiratory cycle (T_{TOT}, s) in adult conscious control and nGHR knockout mice under normoxia (FiO_2 = 0.21) or hypercapnic condition ($FiCO_2$ = 0.07). N = 6/group; Two-way ANOVA; p > 0.05.

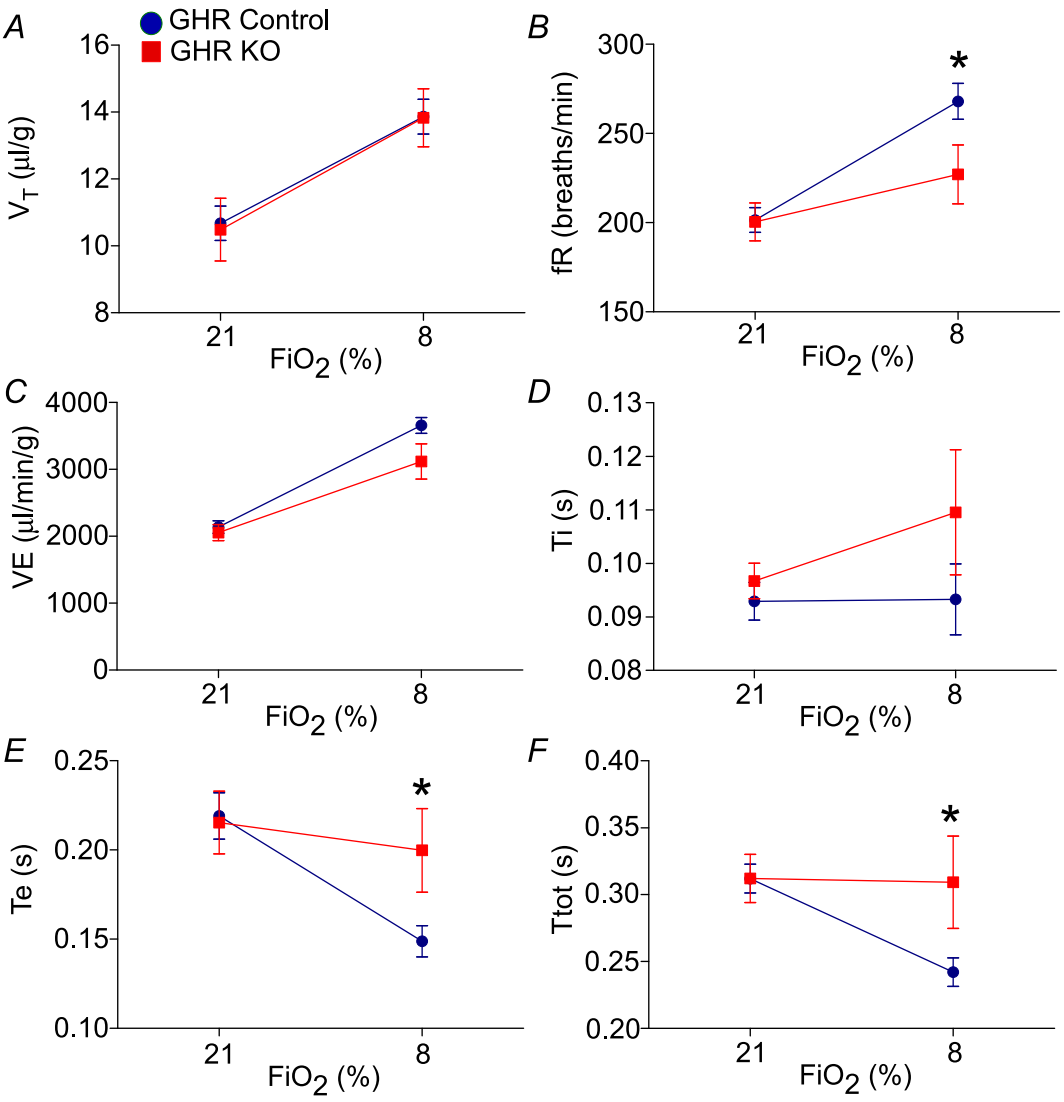

Fig. 4. GHR knockout mice affect the tachypneic response to hypoxia *in vivo.* Changes in A) tidal volume (V_T, µl/g); B) respiratory rate (f_R, breaths/min); C) minute ventilation (V_E, µl/min/g); D) inspiratory time (T_I, s); E) expiratory time (T_E, s), and F) total respiratory cycle (T_{TOT}, s) in adult conscious control and nGHR knockout mice under normoxia ($FiO_2 = 0.21$) or hypoxic condition ($FiO_2 = 0.08$). *Different from GHR control N = 9/group; Two-way ANOVA; $p < 0.05$.

3.3. Hypoxia-mediated activation of catecholaminergic neurons in the NTS and C1 region is not affected in nGHR KO mice

Since a reduction in the tachypneic response to hypoxia was observed in nGHR KO mice, the following experiment was designed to investigate if acute hypoxia exposure affects the expression of a marker of neuronal activation, the Fos protein, within the NTS, C1 region, LC, and PVH. In this experiment, approximately 15-week-old male mice were used. As expected, acute hypoxia ($FiO_2 = 0.08$) produced a robust activation of neurons located in the NTS, C1 region, LC, and PVH (Figs. 5 and 6). However, we found that deletion of GHR did not affect the number of fos activated cells within the NTS (Fos^+ cells: 110 ± 17, vs. control: 104.3 ± 4, $P = 0.75$) (Fig. 5A–B). We also did not find significant differences between control and nGHR KO mice in the activation of TH-expressing cells in the NTS (A2 region) (Fos^+/TH^+: cells: 18.6 ± 2.6, vs. control: 18 ± 1.6, $P = 1$) (Fig. 5A–B). Additionally, we found no significant differences in the number of fos activated cells within the ventrolateral medulla (Fos^+ cells: 52.3 ± 6.9, vs. control: 67 ± 16.5, $P = 0.45$) (Fig. 5D–F). TH-expressing cells in the ventrolateral medulla (A1 and C1 regions) were not affected by neuronal GHR ablation (Fos^+/TH^+ cells: 78.3 ± 7.3, vs. control: 80 ± 7.2, $P = 0.8$) (Fig. 5F). The number of Fos^+ neurons in motor neurons of the DVMN was also not affected in nGHR KO mice (40.6 ± 11.2, vs. control: 42 ± 7.5, $P = 0.9$) (Fig. 5C).

The number of fos activated cells in the LC (Fos^+/TH^+ cells: 102.7 ± 18.8, vs. control: 95.6 ± 33.9, $P = 0.8$) or in the PVH (Fos^+ cells: 629.3 ± 65.7, vs. control: 634.7 ± 32, $P = 0.9$) was also not affected in nGHR KO mice (Fig. 6A–D).

3.4. GH secretion tends to be suppressed during hypoxia

To test whether GH secretion was affected during hypoxia, we measured blood GH levels in 12-week-old C57BL/6 male mice before (normoxia - $FiO_2 = 0.21$) and after 10 min of hypoxia ($FiO_2 = 0.08$). Although we observed a tendency of hypoxia to reduce blood GH levels in mice (3.23 ± 2.73 ng/mL, vs. normoxia: 7.34 ± 5.83 ng/mL; p = 0.06), no significant levels were observed (Fig. 7).

4. Discussion

The present study determined for the first time whether GHR signaling in neurons affects breathing under resting conditions and during challenges such as hypoxia and hypercapnia. The significant findings of this study were the presence of GH-responsive neurons in areas involved in the control of breathing and, especially, the discovery

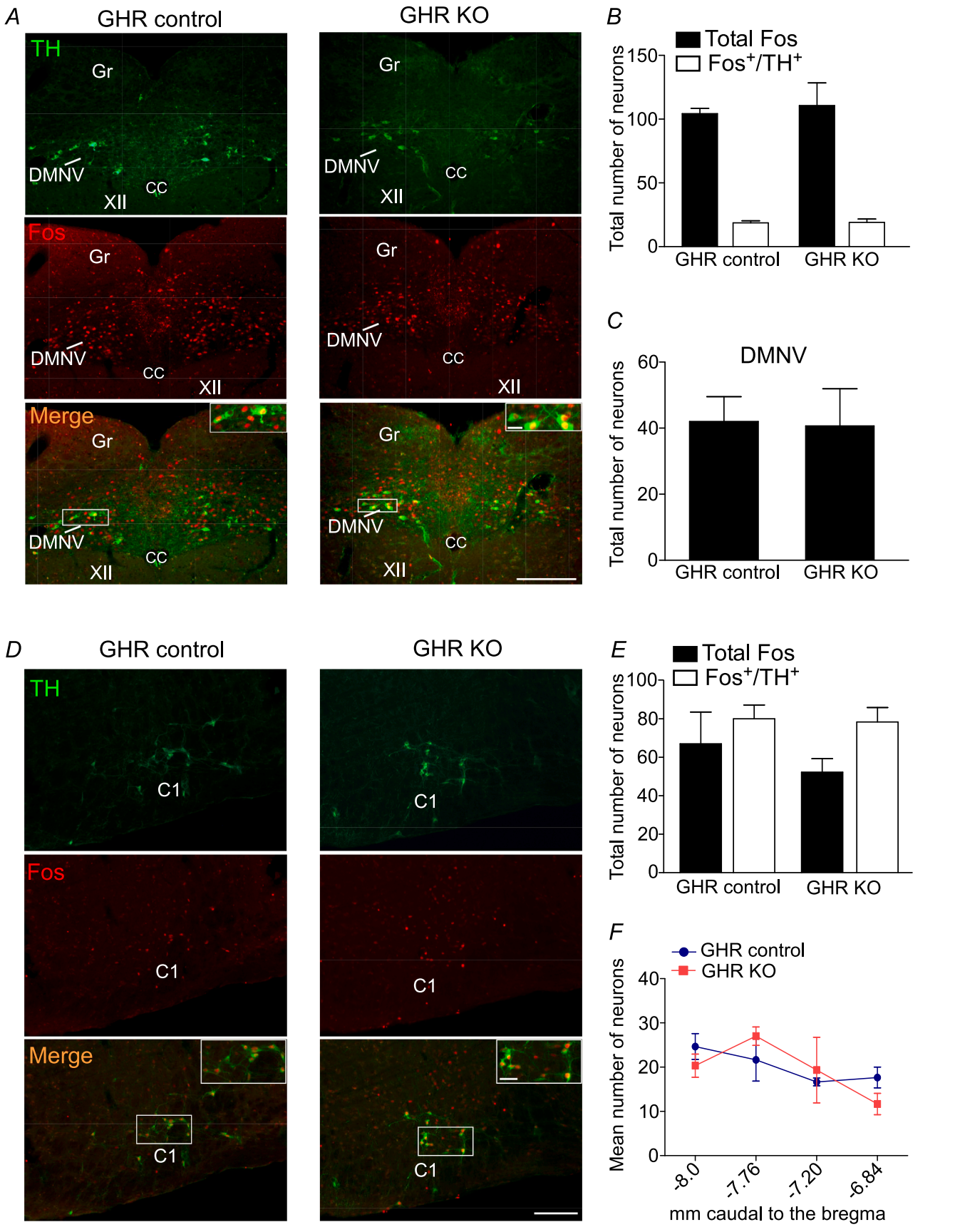

(caption on next page)

Fig. 5. Hypoxia-activated brainstem neurons in mice. A) Photomicrograph of a coronal section of the nucleus of the solitary tract (NTS) showing, Fos, and double-immuno staining. The enlarged picture (inset) demonstrated the presence of TH (red) and Fos (green) within the NTS. B) Total number of Fos/TH-immunoreactive neurons in the NTS in control and nGHR knockout mice. c) Total number of Fos-immunoreactive neurons in the dorsal motor nucleus of the vagus (DMNV) in control and GHR knockout mice. D) Photomicrograph of a coronal section of the rostral ventrolateral medulla (RVLM) showing TH, Fos, and double-immuno staining. The enlarged picture (inset) demonstrated the presence of TH (green) and Fos (red) within the RVLM. E) Total number of Fos/TH-immunoreactive neurons in the RVLM in control and nGHR knockout mice. F) Rostrocaudal distribution of the total number of Fos/TH-immunoreactive neurons in the RVLM plotted as a function of distance from bregma. Scale bar: 0.5 mm in A (lower panel) (applied to all panels); 20 μm in the enlarged picture of the dorsal brainstem; 0.5 mm in B (lower panel) (applied to all panels); 40 μm in the enlarged picture of the ventral brainstem. N = 4/group. Abbreviations: Abbreviations: cc, central canal; DVMN, dorsal vagus motor nucleus; GR, gracil nucleus; XII, hypoglossal motor nucleus. (For interpretation of the references to colour in this figure legend, the reader is referred to the web version of this article.)

that the absence of GHR in neurons is sufficient to reduce the tachypneic ventilatory response to hypoxia. Despite these findings, we did not observe significant differences in the number of hypoxia-activated cells in the NTS, C1 region, LC, and PVH, key regions that are activated under hypoxia and contain GH-responsive cells. These data support a significant, although the secondary role of central GH action in the tachypneic response to hypoxia in conscious mice.

4.1. GH action in the brain to regulate breathing

Recent findings indicate that GH-responsive neurons are found in brainstem areas involved in breathing regulation such as the ventrolateral medulla (RTN and C1 region), NTS, and LC (Furigo et al., 2017; Wasinski et al., 2021; present results). The widespread distribution of GH-responsive neurons in the brain suggests a broad array of neural functions that can be modulated by the direct action of GH, including breathing. Therefore, we tested whether a neuron-specific KO mouse presents alterations in breathing regulation. Our experiments demonstrated that the absence of GHR in neurons affected the tachypneic response to hypoxia, although no changes were observed when nGHR KO mice were exposed to hypercapnia. These functional data prompt us to investigate the neuronal activation in key brain areas that is well described to be active under hypoxia. As expected, hypoxia produced fos expression in all brain areas (RTN, C1, NTS, LC, and PVN) investigated. However, in these neurons, elimination of GHR did not affect the number of hypoxia-activated cells. The reasons for the discrepancies are unclear. For instance, subtle differences in neuronal activity may not be detected via fos expression. Thus, this method may not have been sensitive enough to detect small, but physiologically relevant differences in cell activity between control and nGHR KO mice. We also examined fos expression at the only one-time point and we exposed the mice to an O_2 level of 8%, conditions that may not have triggered maximal changes in GH secretion. Accordingly, only a tended was observed in the reduction in blood GH levels in mice exposed to hypoxia level of 8%. In line with our findings, a previous study has found that acute hypoxia caused decreased plasma GH and increased pituitary GH content in rats (Zhang and Du, 2000). Furthermore, 25-day hypoxia exposure leads to a reduction in body growth and GH secretion. Thus, future studies are necessary to investigate whether more severe or chronic hypoxic conditions in mice may depend more on central GHR signaling. It is also important to point out that our data demonstrated that chemosensors within the brainstem such as the Phox2b-expressing neurons and astrocytes are not responsive to GH. Both the phox2b neurons and GFAP-expressing astrocytes in the ventrolateral medulla were described to be enrolled in breathing regulation (Stornetta et al., 2006; Takakura et al., 2014; Sobrinho et al., 2017; Sheikhbahaei et al., 2018; Czeisler et al., 2019; Moreira et al., 2021).

The brainstem areas investigated in the present study are not under the modulation of GH and additional structures such as the rhythm generator neurons (PreBotzinger complex) could be more sensitive to GH and have a significant role in breathing regulation. Because we found a reduction in the tachypneic response to hypoxia, we suspect that GH has a role in the rhythm neural activity in the preBötC. The preBötC was initially defined as the region of the ventrolateral medulla necessary and sufficient to generate inspiration-related rhythm and respiratory motor output (Del Negro et al., 2018). Most breathing-related preBötC neurons show activity in phase with inspiration (Smith et al., 1991). Thus, future studies are still necessary to confirm the role of GH on preBötC neurons.

From a translational standpoint, the Prader-Willi syndrome (PWS) is a rare genetic disorder caused by the absence of expression of the paternal alleles. Obesity and hormonal deficiencies, especially GH, are the most important signs from the therapeutic viewpoint. In this regard, a previous study has found that GH treatment in PWS patients increases arterial oxygenation during sleep. No changes in breathing stability, ventilation, heart rate, and pulse transit time were observed, although an improvement in the coupling between heart rate and pulse transit time was found after GH therapy (Katz-Salamon et al., 2012). Individuals with PWS have absent peripheral chemoreceptor function (Gozal et al., 1994; Katz-Salamon et al., 2012). Because we found no change in brainstem areas related to chemoreceptor function, it is possible that a disruption in the carotid body can account for the ventilatory response to hypoxia as already demonstrated in humans (Gozal et al., 1994).

4.2. Caveats and experimental limitations

There is considerable evidence that the nGHR KO mice have significant changes in body growth/acromegaly, once these mice lose the central feedback that regulates GH secretion and therefore hypersecrete GH and thus have greater body growth (Furigo et al., 2019; Wasinski et al., 2020; Wasinski et al., 2021; Donato et al., 2021). It is possible that these body changes can affect breathing activity. GH oversecretion enhances ventilation which has been attributed to an increase in the size and/or the number of alveoli (Brody et al., 1970; Iandelli et al., 1997). However, peripheral mechanisms are not the major determinant of breathing regulation. In the present study, we did not find changes in the baseline ventilation nor in the HCVR, while the tachypneic response to hypoxia was reduced. This agrees with the literature of acromegaly patients that the ventilatory response to CO_2 was within the normal range, while the response slopes to hypoxia were low (Grunstein et al., 1994; Iandelli et al., 1997). Future studies are necessary to investigate respiratory mechanics parameters to have a clear view of the control of breathing. Furthermore, our mouse model affected GHR signaling only in neurons and glial cells play a key role in the central control of breathing. Besides brain mechanism, peripheral (muscular) factors appear to influence the ventilatory control and modulate the central motor output. Finally, since genetic GHR deletion occurred in nestin-expressing cells, which represent neural progenitor cells, this early ablation may have favored the development of compensatory mechanisms that mask the actual participation of central GH signaling in the control of breathing. Thus, future models that allow late manipulations in the expression of GHR may represent more specific tools to understand the central functions of GH.

5. Conclusions

Our finding that GH did not impact baseline ventilation and has a minor contribution to breathing stimulation under hypoxia is somewhat surprising given that GH reportedly does increase ventilatory

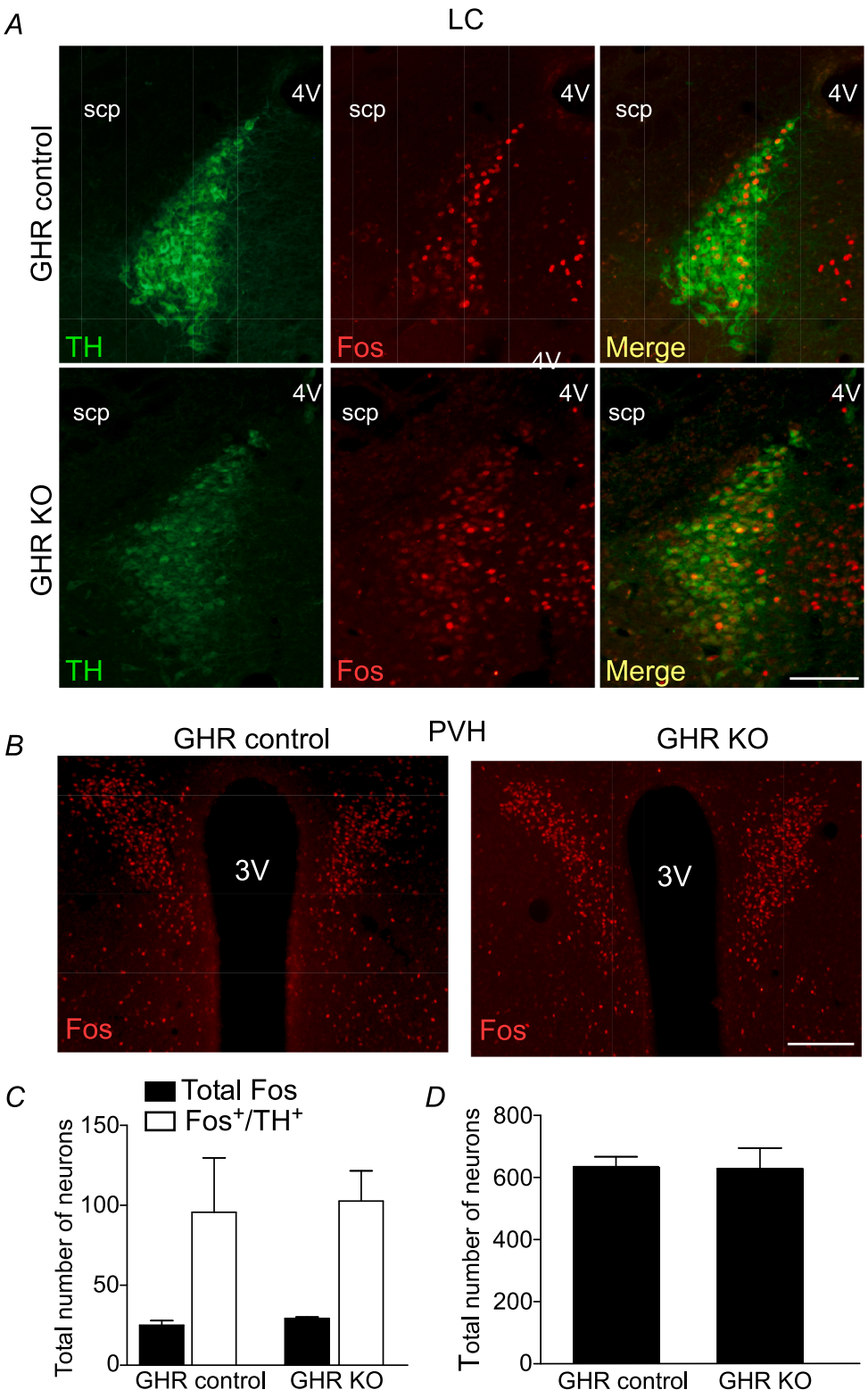

Fig. 6. Hypoxia-activated locus coeruleus and hypothalamic neurons in mice. A) Photomicrograph of a coronal section of the locus coeruleus (LC) showing TH (green), Fos (red), and double-immuno staining (orange). B) Photomicrograph of a coronal section of the paraventricular nucleus of the hypothalamus showing fos immunoreactive (red). C) Total number of Fos/TH-immunoreactive neurons in the LC in control and nGHR knockout mice. D) Total number of Fos-immunoreactive neurons in the PVH in control and nGHR knockout mice. Scale bar: 100 μm in A (lower panel) (applied to all panels); 200 μm in b (lower panel) (applied to all panels). N = 4/group. Abbreviations: scp; spinocerebellar tract; 3 V, third ventricle; 4 V, fourth ventricle. (For interpretation of the references to colour in this figure legend, the reader is referred to the web version of this article.)

chemoreceptor responsiveness during wakefulness (Lindgren et al., 1999). This finding suggests that GH either (i) does not directly influence central and/or peripheral chemoreceptor function or (ii) its effects are state-dependent. The receptors for GH are widespread throughout the CNS (Furigo et al., 2017; Wasinski et al., 2021), including the brainstem; however, here we showed that they are not expressed in neuronal profile directly involved in breathing automaticity and chemoreception. Alternatively, it is possible that wakefulness exerts a profoundly stimulatory effect on breathing influencing the respiratory center in the brainstem (Saper et al., 1976; Geerling et al., 2010). It is conceivable that the reported minor effect on breathing by removing GHR during wakefulness may simply be a general stimulatory action of GH on forebrain structures rather than a direct effect on medullary and/or peripheral chemoreceptors per se.

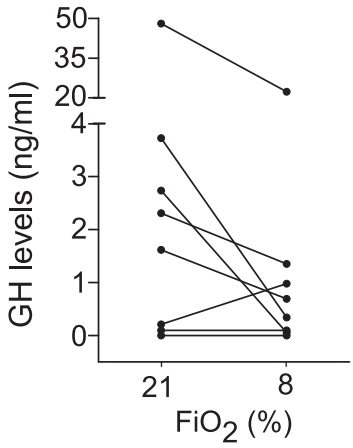

Fig. 7. GH secretion during hypoxia. Blood GH levels before (normoxia - FiO_2 = 0.21) and after 10 min of hypoxia (FiO_2 = 0.08) in C57BL/6 male mice.

6. Data availability statement

The data that support the findings of this study are available from the corresponding author upon reasonable request.

Declaration of Competing Interest

The authors declare that they have no known competing financial interests or personal relationships that could have appeared to influence the work reported in this paper.

Acknowledgments

This work was supported by the São Paulo Research Foundation (FAPESP; grants: 2016/20897-3 to FW; 2020/01318-8 to JD; 2015/23376-1 to TSM). FAPESP fellowship (2017/12678-2 to TMS; 2018/13707-9 to KCF). CNPq fellowship (303363/2019-3 to JD; 302288/2019-8 to ACT and 302334/2019-0 to TSM). This study was financed in part by the Coordenação de Aperfeiçoamento de Pessoal de Nível Superior – Brasil (CAPES) – Finance Code 001.

References

Ashhad, S., Kam, K., Negro, C.A.D., Feldman, J.L., 2022. Breathing Rhythm and Pattern and Their Influence on Emotion. Annu. Rev. Neurosci. 45 (1).
Bartlett Jr, D., Tenney, S.M., 1970. Control of breathing in experimental anemia. Respir. Physiol. 10 (3), 384–395.
Berquin, P., Bodineau, L., Gros, F., Larnicol, N., 2000. Brainstem and hypothalamic areas involved in respiratory chemoreflexes: a Fos study in adult rats. Brain Res. 857, 30–40.
Brody, S.J., Fisher, A.B., Gocmen, A., DuBois, A.B., 1970. Acromegalic pneumomegaly: lung growth in the adult. J. Clin. Invest. 49, 1051–1060.
Czeisler, C.M., Silva, T.M., Fair, S.R., Liu, J., Tupal, S., Kaya, B., Cowgill, A., Mahajan, S., Silva, P.E., Wang, Y., Blissett, A.R., Göksel, M., Borniger, J.C., Zhang, N., Fernandes-Junior, S.A., Catacutan, F., Alves, M.J., Nelson, R.J., Sundaresean, V., Rekling, J., Takakura, A.C., Moreira, T.S., Otero, J.J., 2019. The role of PHOX2B-derived astrocytes in chemosensory control of breathing and sleep homeostasis. J. Physiol. 597 (8), 2225–2251.
Del Negro, C.A., Funk, G.D., Feldman, J.L., 2018. Breathing matters. Nat. Rev.Neurosci. 19 (6), 351–367.
Donato Jr, J., Wasinski, F., Furigo, I.C., Metzger, M., Frazão, R., 2021. Central Regulation of Metabolism by Growth Hormone. Cells 10 (1), 129.
Dos Santos, W.O., Gusmao, D.O., Wasinski, F., List, E.O., Kopchick, J.J., Donato Jr., J., 2021. Effects of Growth Hormone Receptor Ablation in Corticotropin-Releasing Hormone Cells. Int. J. Mol. Sci. 22 (18), 9908.
Furigo, I.C., Metzger, M., Teixeira, P.D., Soares, C.R., Donato Jr., J., 2017. Distribution of growth hormone-responsive cells in the mouse brain. Brain Struct. Funct. 222 (1), 341–363.
Furigo, I.C., Teixeira, P.D.S., de Souza, G.O., Couto, G.C.L., Romero, G.G., Perello, M., Frazao, R., Elias, L.L., Metzger, M., List, E.O., Kopchick, J., Donato Jr., J., 2019. Growth hormone regulates neuroendocrine responses to weight loss via AgRP neurons. Nat. Commun. 10, 662.
Geerling, J.C., Shin, J.W., Chimenti, P.C., Loewy, A.D., 2010. Paraventricular hypothalamic nucleus: axonal projections to the brainstem. J. Comp. Neurol. 518 (9), 1460–1499.
Gozal, D., Arens, R., Omlin, K.J., Ward, S.L., Keens, T.G., 1994. Absent peripheral chemosensitivity in Prader-Willi syndrome. J. Appl. Physiol (1985) 77 (5), 2231–2236.
Grunstein, R.R., Ho, K.Y., Berthon-Jones, M., Stewart, D., Sullivan, C.E., 1994. Central sleep apnea is associated with increased ventilatory response to carbon dioxide and hypersecretion of growth hormone in patients with acromegaly. Am. J. Respir. Crit. Care Med. 150 (2), 496–502.
Guyenet, P.G., Bayliss, D.A., 2015. Neural Control of Breathing and CO2 Homeostasis. Neuron 87 (5), 946–961.
Iandelli, I., Gorini, M., Duranti, R., Bassi, F., Misuri, G., Pacini, F., Rosi, E., Scano, G., 1997. Respiratory muscle function and control of breathing in patients with acromegaly. Eur. Respir. J. 10 (5), 977–982.
Katz-Salamon, M., Lindgren, A.C., Cohen, G., 2012. The effect of growth hormone on sleep-related cardio-respiratory control in Prader-Willi syndrome. Acta Paediatr. 101 (6), 643–648.
King, T.L., Ruyle, B.C., Kline, D.D., Heesch, C.M., Hasser, E.M., 2015. Catecholaminergic neurons projecting to the paraventricular nucleus of the hypothalamus are essential for cardiorespiratory adjustments to hypoxia. Am. J. Physiol. (Regul. Integr. Comp. Physiol.) 309(7), R721-R731.
Lanfranco, F., Motta, G., Minetto, M.A., Ghigo, E., Maccario, M.J., 2010. Growth hormone/insulin-like growth factor-I axis in obstructive sleep apnea syndrome: an update. Endocrinol. Invest. 33 (3), 192–196.
Li, R.C., Guo, S.Z., Raccurt, M., Moudilou, E., Morel, G., Brittian, K.R., Gozal, D., 2011. Exogenous growth hormone attenuates cognitive deficits induced by intermittent hypoxia in rats. Neuroscience 196, 237–250.
Lindgren, A.C., Hellström, L.G., Ritzén, E.M., Milerad, J., 1999. Growth hormone treatment increases CO(2) response, ventilation and central inspiratory drive in children with Prader-Willi syndrome. Eur. J. Pediatr. 158 (11), 936–940.
List, E.O., Berryman, D.E., Funk, K., Gosney, E.S., Jara, A., Kelder, B., Wang, X., Kutz, L., Troike, K., Lozier, N., Mikula, V., Lubbers, E.R., Zhang, H., Vesel, C., Junnila, R.K., Frank, S.J., Masternak, M.M., Bartke, A., Kopchick, J.J., 2013. The role of GH in adipose tissue: lessons from adipose-specific GH receptor gene-disrupted mice. Mol. Endocrinol. 27 (3), 524–535.
Malan, A., 1973. Ventilation measured by body plethysmography in hibernating mammals and in poikilotherms. Respir. Physiol. 17 (1), 32–44.
Moreira, T.S., Sobrinho, C.R., Falquetto, B., Oliveira, L.M., Lima, J.D., Mulkey, D.K., Takakura, A.C., 2021. The retrotrapezoid nucleus and the neuromodulation of breathing. J. Neurophysiol. 125 (3), 699–719.
Nair, D., Ramesh, V., Li, R.C., Schally, A.V., Gozal, D.J., 2013. Growth hormone releasing hormone (GHRH) signaling modulates intermittent hypoxia-induced oxidative stress and cognitive deficits in mouse. Neurochemistry 127 (4), 531–540.
Paxinos, G., Franklin, K., 2012. The Mouse Brain in Estereotaxic Coordinates, first ed. Elsevier, United States of America.
Quaresma, P.G.F., Dos Santos, W.O., Wasinski, F., Metzger, M., Donato Jr., J., 2021. Neurochemical phenotype of growth hormone-responsive cells in the mouse paraventricular nucleus of the hypothalamus. J. Comp. Neurol. 529 (6), 1228–1239.
Saper, C.B., Loewy, A.D., Swanson, L.W., Cowan, W.M., 1976. Direct hypothalamo-autonomic connections. Brain Res. 117 (2), 305–312.
Sheikhbahaei, S., Turovsky, E.A., Hosford, P.S., Hadjihambi, A., Theparambil, S.M., Liu, B., Marina, N., Teschemacher, A.G., Kasparov, S., Smith, J.C., Gourine, A.V., 2018. Astrocytes modulate brainstem respiratory rhythm-generating circuits and determine exercise capacity. Nat. Commun. 9 (1), 370.
Silva, T.M., Takakura, A.C., Moreira, T.S., 2016. Acute hypoxia activates hypothalamic paraventricular nucleus-projecting catecholaminergic neurons in the C1 region. Exp. Neurol. 285 (Pt A), 1–11.
Smith, J.C., Ellenberger, H.H., Ballanyi, K., Richter, D.W., Feldman, J.L., 1991. Pre-Bötzinger complex: a brainstem region that may generate respiratory rhythm in mammals. Science 254 (5032), 726–729.
Sobrinho, C.R., Gonçalves, C.M., Takakura, A.C., Mulkey, D.K., Moreira, T.S., 2017. Fluorocitrate-mediated depolarization of astrocytes in the retrotrapezoid nucleus stimulates breathing. J. Neurophysiol. 118 (3), 1690–1697.
Stornetta, R.L., Moreira, T.S., Takakura, A.C., Kang, B.J., Chang, D.A., West, G.H., Brunet, J.F., Mulkey, D.K., Bayliss, D.A., Guyenet, P.G., 2006. Expression of Phox2b by brainstem neurons involved in chemosensory integration in the adult rat. J. Neurosci. 26 (40), 10305–10314.
Takakura, A.C., Barna, B.F., Cruz, J.C., Colombari, E., Moreira, T.S., 2014. Phox2b-expressing retrotrapezoid neurons and the integration of central and peripheral chemosensory control of breathing in conscious rats. Exp. Physiol. 99 (3), 571–585.
Wasinski, F., Furigo, I.C., Teixeira, P.D.S., Ramos-Lobo, A.M., Peroni, C.N., Bartolini, P., List, E.O., Kopchick, J.J., Donato Jr., J., 2020. Growth hormone receptor deletion reduces the density of axonal projections from hypothalamic arcuate nucleus neurons. Neuroscience 434, 136–147.
Wasinski, F., Klein, M.O., Bittencourt, J.C., Metzger, M., Donato Jr., J., 2021. Distribution of growth hormone-responsive cells in the brain of rats and mice. Brain Res. 1751.
Zhang, Y.S., Du, J.Z., 2000. The response of growth hormone and prolactin of rats to hypoxia. Neurosci. Lett. 279 (3), 137–140.